Recovering Human Body Configurations using Pairwise Constraints between Parts

Paper No.: 1400

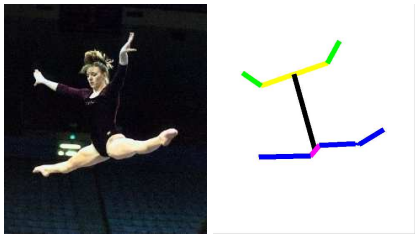

Figure 1: The challenge is to take the input image (a), recover the body configuration in (b).

Abstract

The goal of this work is to recover human body configurations from static images. Without assuming a priori knowledge of scale, pose or appearance, this problem is extremely challenging and demands the use of all possible sources of information. We develop a framework which can incorporate arbitrary pairwise constraints between body parts, such as scale compatibility, relative position, symmetry of clothing and smooth contour connections between parts. We detect candidate body parts from bottom-up using parallelism, and use various pairwise configuration constraints to assemble them together into body configurations. To find the most probable configuration, we solve an Integer Quadratic Programming *problem with a standard technique using linear approximations. Approximate IQP allows us to incorporate much more information than the traditional dynamic programming and remains computationally efficient.* 15 *hand-labeled images are used to train the low-level part detector and learn the pairwise constraints. We show test results on a variety of images.*

1. Introduction

The goal of this work is to take an image such as the one in Figure 1(a), detect a human figure, find the configuration of parts (b). This is a very difficult problem, partly because the pose of human bodies can be extremely versatile, resulting in various aspects or self-occlusions, and partly because the variations in clothing and background clutter denies a simple appearance model.

Given the seemingly insurmountable difficulties, many of the existing approaches to this problem make simplifications of one sort or another, either assuming the knowledge of the scale and appearance/color, or using motion information from video sequences to do background subtraction, or limiting oneself to restricted domains such as walking figures. In these cases, a canonical tree-based model is typically used to model body parts, where dynamic programming can be applied.

We take the challenge to tackle the problem in a more general setting. Without restrictions in pose, appearance or background clutter, as some authors have argued [11], a tree-based model no longer suffices. We need a lot more sources of information to succeed, which a tree-based model cannot accommodate. For example, the symmetry of clothing is a very powerful cue to constrain limb appearance without a prior. For the example in Figure 1, what reveals the body position to us are the connection of the upper legs and the relative geometric relation between arms and legs, both of which are not in the traditional tree-based model.

It is an open question what models are computationally feasible. In this work, we develop a strategy which exploits a rich set of cues, defined on arbitrary pairs of parts, to constrain body configurations. We learn these constraints from empirical data and use *Integer Quadratic Programming* (IQP) to find the most probable configurations. IQP is a well-studied computational framework, where efficient approximations exist. Most of the cues on human body configuration can be expressed as pairwise constraints. In our experiments we have found that IQP works well for this problem. IQP allows us to incorporate much more information than dynamic programming, and we can handle a much larger set of candidate parts than the brute-force search strategy in [11].

The structure of this paper is as follows: In Section 2 we discuss related previous work. In section 3 we summarize our approach. Section 4 describes our bottom-up part detector and 5 provides the details of the pairwise configuration constraints. Section 6 discusses the IQP formulation and its approximations. Experimental results are shown in Section 7 and we conclude in Section 8.

2. Related Work

Finding people is a hard problem; yet it is a problem of great interest to both scientific researchers and engineers. One of the earliest lines of research on this problem is in the limited setting of detecting and tracking pedestrians. Starting with Hogg[5], there has been a lot of work done on using 3D kinematic models for tracking [3]. These 3D models have a high degree of kinematic freedom and typically require hand initialization. Lee and Cohen [7] recently managed to use 3D models to detect people mostly in standing poses, making inference with Data-Driven MCMC.

More recent developments in pedestrian detection typically use a large amount of training data and make clever designs of classifiers, the most successful of which is probably that of Viola et al. [18]. These template-based approaches do not recover joint locations, and have not yet been generalized to accommodate more pose variations.

Realizing the difficulties of using 3D part-based models, many researchers have explored the use of 2D holistic exemplars. Toyama and Blake [17] used exemplars for tracking people as 2D edge maps. Mori and Malik [10], and Sullivan and Carlsson [16] both use 2D exemplars to match and localize human body parts. The main problem with such exemplar-based approach is that it does not have an intrinsic notion of parts, therefore having to deal with the combinatorial explosion when the variations of pose, clothing and clutter increase. Shakhnarovich et al. [13] uses a brute-force approach to attack this complexity explosion, using a variant of Locality Sensitive Hashing to speed up search. However, such an approach still requires millions of exemplars, if not more, even just for the upper body with common poses.

On the other hand, there have been many approaches that explicitly model human body as an assembly of parts. Typically, a low-level detector is applied on the image to extract candidate parts; then a top-down procedure makes inference about the configuration and finds the best assembly. Song et al. [15] detect corner features in video sequences and model their joint statistics using a tree models. Felzenswalb and Huttenlocher [2] uses the distance transform to perform dynamic programming, again on the canonical tree model. Ioffe and Forsyth [6] use a simple rectangle detector to find candidates and assemble them by sampling based on kinematic constraints on a mixture of tree models.

The recent paper of Mori et al. [11] is the most relevant to our work. We follow a similar strategy, i.e., detecting candidate parts from bottom-up, and then assemble the candidate parts using configuration constraints. We both realize the limitations of tree-based models. Their work mainly focus on low-level processing, aiming at using sophisticated techniques such as Normalized Cuts to find a few salient body parts. They solve the assembly problem by brute-force search. Instead, we will use a relative simple low-level detector, and solve the assignment problem using IQP, which can systematically explore arbitrary pairwise constraints.

3. Our Approach

The ultimate goal of our line of research is to develop a general method to recover configurations of human bodies, or other articulated objects, from static images. What characterizes an articulated object is that the object is made of a collection of simple rigid parts that are constrained under a global configuration. It is self-evident, therefore, that any approach without explicitly modeling the part structure would have great difficulties in handling pose variation, appearance change or background clutter.

There are in general two ways to detect parts of articulated objects: top-down and bottom-up. A typical top-down approach is to design rectangle-like filters or templates that model the shape of each object part, and match them to every possible location in the image. Such template matching is useful if one knows a priori the scale and the appearance of what he looks for. Because we aim at finding people in a general setting, this would require us to run part detectors at multiple scales, orientations, and aspect ratios (e.g., to account for foreshortening). We would find far too many candidate parts to be efficiently searched and assembled at a later stage.

Our approach to finding people is to first detect candidate body parts from bottom-up, and then search for the combination of the candidate parts that is most probable for human bodies. Figure 2 shows an example of how information flows through various stages of the process:

Starting with the input image in Figure 2(a), we use the local Pb operator [9] to compute a soft edge map in Figure 2(b). We use Canny's hysteresis to convert the soft edge map into contours, and recursively split them into piecewise straight lines. We then use *Constrained Delaunay Triangulation* (CDT) to complete this scale-invariant discrete line structure into a triangulation (Figure 2(c)).

We model a body part by a pair of parallel lines and build a discriminative part detector on the basis of the CDT triangulation. For each pair of edges in the triangulation, we use a logistic classifier to compute its low-level saliency as a body part. The logistic classifier is trained from 15 images extracted from a skating sequence performed by Tara Lipinski with hand-labeled parts.

Figure 2(d) shows the candidate parts detected in this image. As we can see, without the knowledge of scale or appearance, our part detector is fairly weak; there are a lot of false detections. After all, parallelism is a generic mid-level cue, and body parts by themselves are not distinctive. It is the configuration of parts that is distinctive for human bodies.

In Section 5 we define a variety of configuration con-

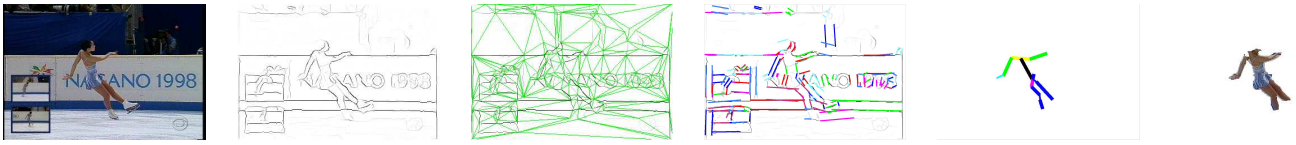

(a) (b) (c) (d) (e) (f)

Figure 2: The processing pipeline: given an input image **(a)**, compute an edge map **(b)**, break this into segments and compute a Constrained Delaunay Triangulation **(c)**, identify part candidates by exploiting parallelism of part boundaries**(d)**, find a good configuration using Integer Quadratic Programming over pairwise constraints between body parts **(e),** use the labled segments and stick figure to find an approximate segmentation of the figure **(f)**

straints between pairs of parts. They go beyond the traditional tree-based model and incorporate constraints such as the compatibility of part width, the symmetry of appearance, and smooth connectivity between parts. We learn the pairwise constraints from the same 15 hand-labeled Lipinski images.

To recover human body configuration is to assign part labels to detected candidate parts. Assuming that the pairwise constraints are independent, these constraints can be formulated as a quadratic cost function for the assignment problem. Hence we can compute the most probable body configurations as solving an *Integer Quadratic Programming* (IQP) problem. The IQP problem is solved by using an efficient linear approximation scheme to IQP [8, 1]. Once we have found the most probably configuration in Figure 2(e), it is straightforward to find the associated segmentation mask shown in Figure 2(f).

We show experimental results on a variety of images.

4. Finding Body Parts

We choose to detect candidate human body parts from bottom-up. Our approach is based on the following key observation: parts of a human body, or of an articulated object in general, are mostly characterized by a pair of parallel line segments. *Parallelism* or *Ebenbreite*, known from the early days of the Gestalt movement, is a fundamental and powerful principle in human vision. It is common understanding that, being a mid-level cue, the perception of parallelism occurs early in the visual pathway. Our approach here follows this theory: first we construct a discrete structure of edges in an image by grouping them into approximately straight contour elements. Then we use *Constrained Delaunay Triangulation* to complete the gaps between contour elements. Finally we train a classifier on a pair of contour elements to compute the probability of them forming the boundary of a body part.

4.1. Constrained Delaunay Triangulation

As the first step of our bottom-up processing, we use the local Pb operator [9] to compute a soft edge map. We use Canny's hysteresis trick to trace high Pb edges in the image into continuous contours. We then recursively split these contours into pieces, until each contour element is approximately straight. This process gives us a discrete graph, the elements of which are straight contours of high Pb edges. We note that this discretization step is scale-invariant: a straight line, no matter how long it is, remains a single line in the graph.

We use *Constrained Delaunay Triangulation* to complete gaps between the detected contour elements. The standard *Delaunay triangulation* (DT) is the dual of Voronoi diagrams and is the unique triangulation of a set of vertices in the plane such that no vertex is inside the circumcircle of any triangle. The constrained Delaunay triangulation (CDT) is a variant of of the DT in which a set of user-specified edges must lie in the triangulation. The CDT retains many nice properties of DT and is widely used in geometric modeling and finite element analysis.

We use the TRIANGLE program [14] to produce CDTs as shown in Figure 2(c). The linearized edges extracted from the Pb contours become constrained edges in the triangulation which we refer to as gradient edges or G-edges (black), and the rest are the completions by the CDT algorithm, what we refer to as C-edges (green).

4.2. Finding Parallel Line Segments

We detect candidate body parts by finding well-aligned parallel lines in the CDT graph. Consider a pair of contour elements (Figure 3): let L denote the length of a contour element, α its orientation, $\vec{C}$ its center, and Pb the average contrast on this element. Let $\vec{T}$ denote the average tangent direction and $\vec{N}$ the normal direction. We define the following set of features:

1. orientation consistency, the difference in orientation $|\alpha_1 - \alpha_2|$; they should have the same orientation;
2. length consistency, $|L_1 - L_2|/(L_1 + L_2)$; they should have the same length;
3. low-level contrast, $|Pb_1 + Pb_2|$ and $|Pb_1 - Pb_2|$; the contrast should be high and the difference should be small;

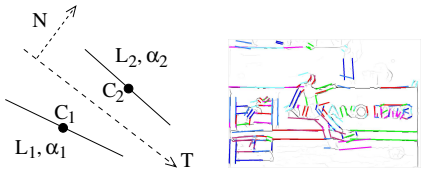

(a) (b)

Figure 3: (a) Classifying parallel line segments. (b) All candidate parts detected in one image.

4. distance between their centers in the normal direction, $|(\vec{C}_1 - \vec{C}_2) \cdot \vec{N}|/(L_1 + L_2)$; this distance should be small;

5. distance between their centers in the tangent direction; $|(\vec{C}_1 - \vec{C}_2) \cdot \vec{T}|/(L_1 + L_2)$; this distance should be small too;

6. intervening contour Pb_{IC}: consider a straight line connecting $\vec{C}_1$ to $\vec{C}_2$ and let Pb_{IC} be the maximum Pb contrast on edges intersecting this path [1]; Pb_{IC} should be close to zero.

We train a simple logistic classifier to combine these features. For training, we use the hand-labeled body parts in the Lipinski dataset as positive examples. As for negative examples, we use all pairs of contour elements whose centers are sufficiently close ($<= 5$ hops in the CDT graph).

Most of the pairs of lines in the graph are unlikely to be body parts: either they are not parallel or too far away from each other. Hence we take a simplifying step that for each line e in the CDT graph, we find the pair (e, e') such that e' is the best match to e, and we only keep (e, e') as a candidate body part. Figure 3(b) shows all the candidate parts found in the image. We note that the candidate parts are very different in scale and aspect ratio: given a pair of edges in the CDT graph, scale and aspect ratio are automatically determined. Therefore in our bottom-up detection step, there is no need to explicitly search over all possible scales and aspect ratios; and while a top-down rectangle detector would fire many times on the long parallel bars in the background, we only find one candidate part and its aspect ratio is wrong for human bodies.

5. Configuration Constraints

Most of the existing approaches model the human body as a tree of parts. The typical configuration constraints used in a tree model are positional and orientation constraints between adjacent parts, such as $torso$-$upperlimb$ connection, or $upper$-$lowerlimb$ connection. These are, however, only a small subset of the information that is available for recovering human body configurations.

One important cue missing from the tree model is the symmetry of clothing: corresponding parts, such as the two forearms, are usually clothed in the same way and thus similar in color. This cue can be very useful in identifying arm positions. Another example is the connectivity between two upper legs. They form a stereotypical "V"-shape, which is typically very salient and heavily exploited by the human visual system. There are many other useful cues between a pair of body parts.

5.1. Constraints between Parts

What is a good configuration? Individual parts have to be consistent with the global configuration. We approximate the global configuration consistency by defining pairwise constraints between parts.

Let c be a candidate part (two parallel lines) detected from the image, and l be a part label (e.g., left upper leg). There are some simple unary constraints on this assignment (l, c):

1. **aspect ratio** $f_{aspect}(l, c)$: anthropometric data [12] provides us constraints on the aspect ratio of each individual part. Parts can be and often are foreshortened; however, the aspect ratio $length/width$ can only be smaller, but not much larger, than the expected aspect ratio;

2. **low-level score** $f_{lowlevel}(c)$: for a candidate part c, we have a measure of the low-level saliency c from the part detector, i.e., the posterior $P_{lowlevel}(c)$ from the logistic classifier. We use $f_{lowlevel}(c) = \log(P_{lowlevel}(c))$.

The unary constraints are very weak in nature. Without knowing the global scale or its relations to other parts, a candidate part can almost be labeled as anything one wants, e.g., a torso or a lower leg. More importantly for recovering configurations are the constraints between parts. We define the following set of cues between a pair of assignments (l_1, c_1) and (l_2, c_2):

1. **scale consistency** $f_{scale}(l_1, c_1, l_2, c_2)$: body parts are roughly speaking cylindrical. Therefore, although *length* is unreliable because of foreshortening, *width* is a good estimate of the global object scale. Let $w_1 = width(c_1)$ and $w_2 = width(c_2)$, compute the ratio $r = (w_1 - w_2)/(w_1 + w_2)$; we compare r to $\tilde{r} = (\tilde{w}_1 - \tilde{w}_2)/(\tilde{w}_1 + \tilde{w}_2)$, where $\tilde{w}_1 = width(l_1)$ and $\tilde{w}_2 = width(l_2)$ are the "expected" widths of these two part labels, as given in anthropometric statistics;

2. **appearance consistency**: the appearance of corresponding parts are similar; this constraint is valid for certain pairs of parts, e.g., between upper legs and between lower legs. Let (L, A, B) be the average color

[1] For simplicity we approximate this straight line by computing the shortest path between C_1 and C_2 in the CDT graph.

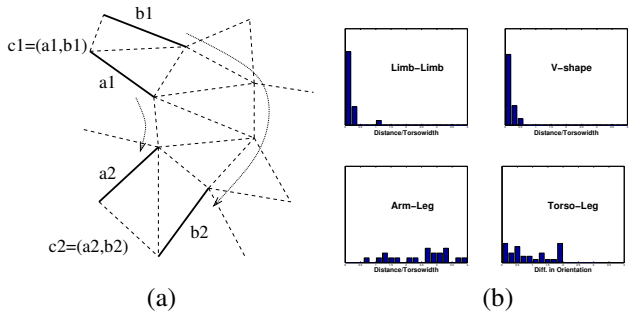

(a) (b)

Figure 4: (a) Defining pairwise constraints on parts. (b) Empirical distributions of distance constraints from training data.

of a part, we compute the difference $f_L = |L_1 - L_2|$ and $f_{ab}|(A_1, A_2) - (B_1, B_2)|$.

3. **orientation consistency** $f_{orient}(l_1, c_1, l_2, c_2)$: let α be the orientation of a part, we compute the difference $f_{orient} = |\alpha_1 - \alpha_2|$. This cue is useful mostly for adjacent body parts. Because of the large variations in pose in the training data, the orientation consistency turns out to be a weak cue.

4. **connectivity**: adjacent body parts should be adjacent in the image; this is the most commonly used cue in constraining possible body configurations. However, connectivity means much more. The V-shape constraint between two upper legs is one example. Another one is the connectivity cue between an upper arm and an upper leg, i.e., there is typically a "smooth" contour connecting them through the torso. We discuss more about how to measure this smooth connectivity in the next section.

5.2. Smooth Connections between Parts

To quantify the smoothness of a connection, we compute the shortest path between two parts in the CDT graph (Figure 4(a)), where the path goes through contour elements in the CDT graph G_{CDT} instead of pixels. In the CDT graph, a path could go through G-edges as well as C-edges (gaps). We would like to tolerate small gaps but avoid jumping large distances along C-edges. Therefore, we raise the cost of traveling along a C-edge by a constant ratio (3.0).

We can compute a number of connectivity cues for a pair of edges (a_1, a_2): $dist(a_1, a_2)$, the total distance of the shortest path $a_1 \rightarrow a_2$ (relative to torso width, which we can estimate from the two parts given anthropometric data); $gap(a_1, a_2)$, the total length of C-edges or gaps on this path; $angle(a_1, a_2)$, the maximum change of angle along the path; and $turn(a_1, a_2)$, the number of "turns" or T-junctions along this path (where traveling through a T-junction is counted as a "turn" if it does not go through the pair of edges that form the minimum angle at this junction).

Now consider a pair of candidates c_1 and c_2: each part has two bounding edges, (a_1, b_1) and (a_2, b_2) respectively. We find a correspondence between these two pairs of edges, such that $dist(a_1, a_2)$, the distance between (a_1, a_2), are the minimum of all four combinations; and (b_1, b_2) are the two other edges. Thus we can define two sets of connectivity cues between parts, one from the path $(a_1 \rightarrow a_2)$ and one from $(b_1 \rightarrow b_2)$. Sometimes both of them are very informative, such as the connectivity between an upper leg and the lower leg, as we expect both sides to be well connected. Sometimes only one of them is useful, such as the connectivity between an upper arm and an upper leg.

5.3. Torso-Limb Constraints

Torso has a special role as being the hub that connects all the limbs together.

Most of the constraints here are designed to make the optimization problem easier.

1. Torso orientation $f_{torsoorient}(c)$: we assume that the torso is oriented upward. Let θ be the leaning angle of the candidate part c, we compute $f_{torsoorient} = |tan(\theta)|$;

2. Left/right disambiguation: given a torso candidate c and its two bounding edges a and b, we know which edge is the left side and which is the right side. When we compute the connectivity of the left (or right) limbs to the torso, we only consider the connectivity to the left (or right) side of the torso.

3. Arm-Leg disambiguation: given the torso orientation, we assume that the center of the upper legs cannot be higher (along the torso orientation) than the top of the torso, and the upper arms cannot be lower than the bottom of the torso.

5.4. Learning the Constraints

We use the hand-labeled Lipinski images for training. With such a limited amount of training data, it would be difficult to learn the interactions between all the pairwise constraints. Thus, for simplicity, we assume that the constraints are all independent of each other, and they have a Gaussian distribution. 15 images are sufficient for us to estimate the mean and standard deviation from the empirical data. For some constraints, such as the distance between upper leg and lower leg, we know it should be zero in the ideal case. In such cases we fix the mean of this constraint to be zero.

Figure 4(b) shows a few empirical distributions of distance constraints. The distance between two upper legs (the V-shape) is typically zero or very small. In comparison, the distance between upper legs and upper arms is less reliable and has a high variance. The orientation constraint between torso and upper leg turns out to be weak (in many cases

> 90 degrees), as there are a lot of pose variations in the training images.

Another observation is that these distributions are clearly non-Gaussian. We leave it for future work to build better parametric models for each type of constraints, possibly with more training data.

6. Integer Quadratic Programming

Recovering human body configuration in an image can be formulated as an assignment of body part labels $\{l_i\}$ to candidate body parts $\{c_j\}$. We use the pairwise constraints f_k introduced in the last section to define the "goodness" of an assignment. For each constraint f_k, we model it with a Gaussian distribution with parameters (μ_k, σ_k). Let $\bar{f}_k = (f_k - \mu_k)^2 / \sigma_k^2$. If we assume that all the constraints are independent, the constraints together define a probabilistic model as a product of Gaussians. Finding the maximum likelihood assignment $\pi : \{l_i\} \rightarrow \{c_j\}$ is then equivalent to minimizing the sum:

$$\sum_{l_1, l_2} \sum_k \bar{f}_k \left(l_1, \pi\left(l_1\right), l_2, \pi\left(l_2\right)\right) + \sum_l d((\pi(l_1)) \qquad (1)$$

Where l_i is a part label, and $\pi(l_i)$ is the part candidate assigned to l_i by π. The pairwise constraints are represented by the $\bar{f}_k$'s. Here $\bar{f}_k \left(l_1, \pi\left(l_1\right), l_2, \pi\left(l_2\right)\right)$ might measure the consistency with respect to relative scale of labeling one part candidate as a leg and another as a torso. Note that for some pairs of limbs and features, $\bar{f}_k$ will be zero – for instance $\bar{f}_k$ is zero for all k whenever l_1 is a lower arm, and l_2 is a lower leg. The final sum is over each limb label l where $d\left(\pi(l)\right)$ measures the quality of an individual part candidate.

Integer Quadratic Programming Minimizing equation 1 can be written as an integer quadratic programming problem (IQP). The assignment π is represented by a binary vector x. Each entry x_i indicates whether one particular part candidate $p(i)$ is labeled with a particular part label $l(i)$. In order for x to represent a valid correspondence there is a constraint that for each part label $\hat{l}$, $\sum_{i:l(i)=\hat{l}} x_i = 1$.

We can now write the integer quadratic programming problem:

$$\begin{aligned} \min Q(x) = & x' H x + d' x \quad \text{subject to,} \\ & Ax = b, \quad x \in \{0,1\}^n \end{aligned} \qquad (2)$$

Here H is a matrix representing the pairwise consistency,

$$H(i,j) = \sum_k \bar{f}_k \left(l(i), p(i), l(j), p(j)\right)$$

Similarly we have $c(i) = d(p(i))$. Finally $Ax = b$ expresses the constraints that x represent an assignment as mentioned above.

The binary vector x that minimizes equation 2 corresponds to the assignment that minimizes equation 1 and therefore has the maximum likelihood under our model.

Linear Bound A linear bounding function $L(x)$ is constructed so that $L(x) < Q(x)$ for all x. Note that from this point forward the constraints from equation 2 are assumed, but not written.

$$q_i = \min_x \sum_j H(i,j) x_j \qquad (3)$$

If x_i indicates assigning limb $l(i)$ to candidate $p(i)$, then $q_i + c_i$ is a lower bound for the cost contributed to any assignment mapping $l(i)$ to $p(i)$. Now we can write the bounding function, $L(x) = \sum_i (q_i + c_i) x_i$. Finding the x that minimizes L and the q_i in equation 3 subject to the constraints in equation 2 is simple because the vertices of the constraint polytopes lie only on integer coordinates. As a result the integer linear programming problems can be relaxed to linear programming problems without changing the optima.

This construction follows [8] and [1], and is a standard bound for a quadratic program.

Greedy Search Starting from the assignment that minimizes L we perform a greedy local search considering up to two changes in the assignment at a time. Considering two changes is important in order to move both upper and lower parts of a limb out of a poor configuration.

Complexity Integer quadratic programming can be quite challenging, it is after all an NP-hard problem, but it turns out the instances generated as described above are not so difficult. A simple linear approximation followed by a greedy local search produces quite good results.

There are more complex approximations to IQP, using semidefinite programming (SDP), with guaranteed bounds on approximation error [4]. However, in this work a simple approximation produces results within the approximation bound and with significantly lower time and space complexity than [4].

If n is the length of x then computing the x that minimizes $L(x)$ including computing all of the q_i takes $O(n^2)$ operations with a very small constant. Each gradient descent step requires approximately the same number of operations. As a comparison SDP techniques are polynomial in n^2, effectively many, many times slower as $n \sim 1300$.

7. Experimental Results

We have tested our algorithm on a variety of images, including extracted frames from a skating sequence of Michel Kwan, and other gymnastic images. Examples are shown in

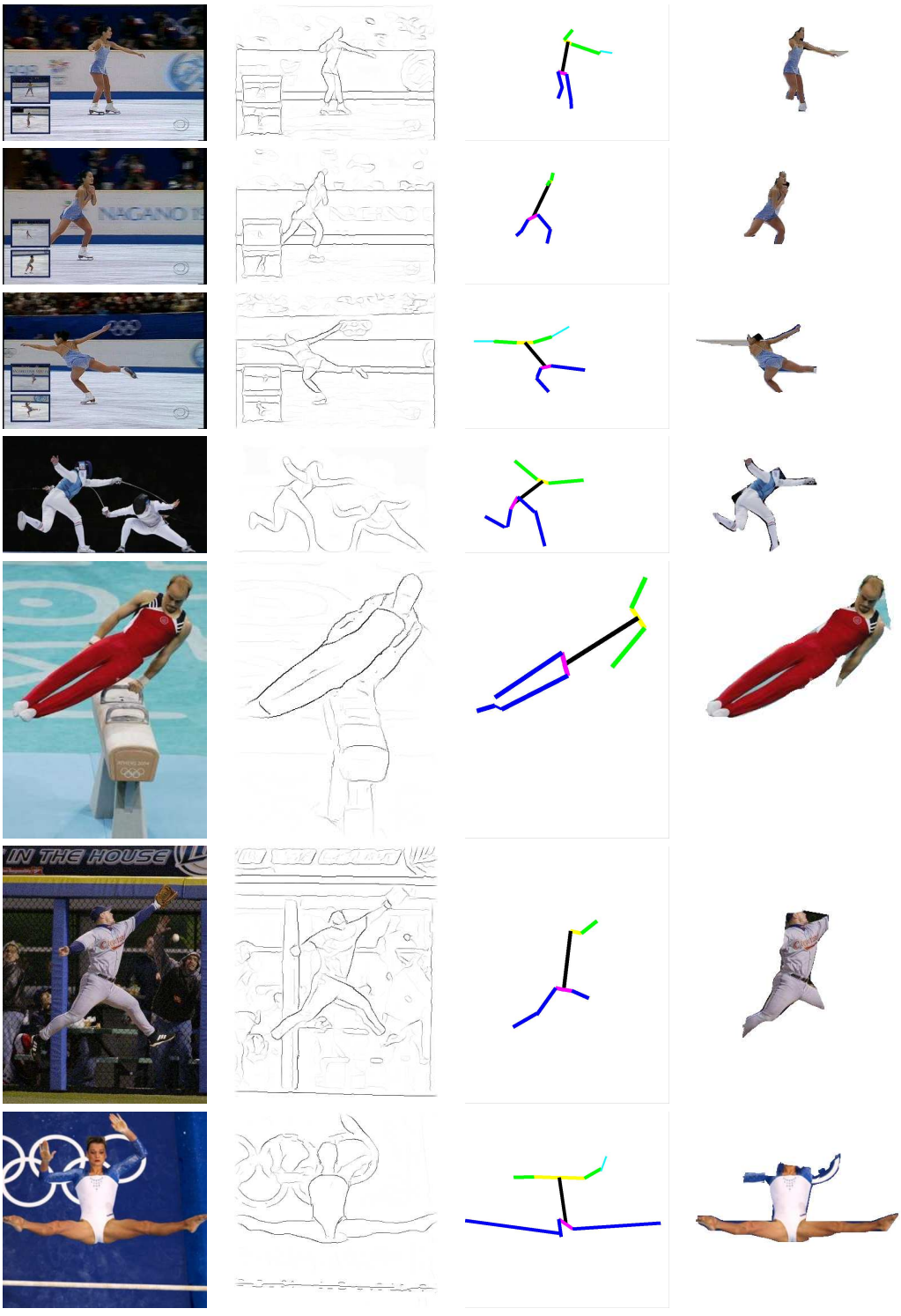

(a) (b) (c) (d)

Figure 7, with recovered body configurations and the associated segmentation masks.

To obtain these results, we use a standard 9-part model for the human body, i.e., torso plus left/right upper/lower legs/arms. The number of candidate parts detected per image is around the range $100 - 200$. We use the set of Gaussian parameters learned from a different skating sequence with a different skater. Because Gaussian models are not very accurate for some features, we choose to "cut off" the features at 4σ; i.e., any cost term above 4σ is considered as being infinity.

Because of the heterogeneous nature of the constraints, our IQP problem is hard to solve. We have found that, occasionally, the linear approximation to IQP fails to locate the correct body parts. The linear approximation step in Equation 3 basically tries to find for each line (or each possible labeling) the best consistent assignment. This is done without considering the pairwise constraints between other parts. Therefore the linear approximation could fail and the gradient descent that followed may not be able to correct the errors.

To remedy this problem, we make use of an empirical observation: that although torsos typically have bad low-level saliency, it is the most constrained part of the body and therefore can be most reliably detected in the linear approximation scheme. We use the following two-step strategy: in the first step, we run the linear approximation to obtain a shortlist of 5 best torso candidates. In the second step, we go through the shortlist, pick one candidate part, fix its label to be the torso and re-solve the IQP problem, with the same cost matrix H. Fixing the torso is appealing because it helps constrain all the upper legs/arms in the configuration. Finally we pick the solution that has the lowest cost Q.

8. Conclusion

In this work we develop a strategy to use pairwise constraints between human body parts to recover body configurations from static images. We detect candidate body parts from bottom-up using parallelism on the basis of a discrete graph structure given by Contrained Delaunay Triangulation. Finding a configuration of human body is then an assignment problem: for each body part, we decide which candidate part we assign the label to. We use *Integer Quadratic Programming* (IQP) to solve the assignment problem.

As compared to the traditional tree-based model and the associated dynamic programming algorithm, IQP allows us to incorporate a much richer set of constraints, namely arbitrary constraints between pairs of body parts. This includes the important cues such as the symmetry of clothing, the canonical V-shape between upper legs, and the smooth contour connectivity between arms and legs. As compared to a brute-force search approach in [11], we are able to handle a much larger set of candidate parts and do not rely on the availability of a few salient ones. We have found that a two-step strategy with the linear approximation of IQP works well for our assignment problem, produces satisfactory results on a variety of images without relying on extensive low-level processing, and are computationally efficient. We believe that IQP will find more and more use in detecting articulated objects.

References

[1] A. Berg, T. Berg, and J. Malik. Shape matching and object recognition using low distortion correspondence. Technical report, UC Berkeley, 2005.

[2] P. F. Felzenszwalb and D. P. Huttenlocher. Efficient matching of pictorial structures. In *Proc. IEEE Comput. Soc. Conf. Comput. Vision and Pattern Recogn.*, 2000.

[3] D. M. Gavrila. The visual analysis of human movement: A survey. *Computer Vision and Image Understanding: CVIU*, 73(1):82–98, 1999.

[4] M. Goemans and D. Williamson. Imroved approximation algorithms for maximum cut and satisfiability problems using semidefinite programming. *acm*, 42(6):1115–1145, 1995.

[5] D. Hogg. Model-based vision: A program to see a walking person. *Image and Vision Computing*, 1(1):5–20, 1983.

[6] S. Ioffe and D. Forsyth. Probabilistic methods for finding people. *Int. Journal of Computer Vision*, 43(1):45–68, 2001.

[7] M. W. Lee and I. Cohen. Proposal maps driven mcmc for estimating human body pose in static images. In *CVPR*, 2004.

[8] J. Maciel and J. Costeira. A global solution to sparse correspondence problems. *PAMI*, 25(2):187–199.

[9] D. Martin, C. Fowlkes, and J. Malik. Learning to find brightness and texture boundaries in natural images. *NIPS*, 2002.

[10] G. Mori and J. Malik. Estimating human body configurations using shape context matching. In *European Conference on Computer Vision*, volume 3, pages 666–680, 2002.

[11] G. Mori, X. Ren, A. Efros, and J. Malik. Recovering human body configurations: Combining segmentation and recognition. In *CVPR*, volume 2, pages 326–333, 2004.

[12] NIST. Anthrokids - anthropometric data of children, http://ovrt.nist.gov/projects/anthrokids/, 1977.

[13] G. Shakhnarovich, P. Viola, and T. Darrell. Fast pose estimation with parameter sensitive hashing. In *Proc. 9th Int. Conf. Computer Vision*, volume 2, pages 750–757, 2003.

[14] J. Shewchuk. Triangle: Engineering a 2d quality mesh generator and delaunay triangulator. In *First Workshop on Applied Computational Geometry*, pages 124–133, 1996.

[15] Y. Song, L. Goncalves, and P. Perona. Unsupervised learning of human motion. *IEEE Trans. PAMI*, 25(7):814–827, 2003.

[16] J. Sullivan and S. Carlsson. Recognizing and tracking human action. In *European Conference on Computer Vision*, volume 1, pages 629–644, 2002.

[17] K. Toyama and A. Blake. Probabilistic exemplar-based tracking in a metric space. In *Proc. 8th Int. Conf. Computer Vision*, volume 2, pages 50–57, 2001.

[18] P. Viola, M. Jones, and D. Snow. Detecting pedestrians using patterns of motion and appearance. In *Proc. 9th Int. Conf. Computer Vision*, pages 734–741, 2003.